Deciphering the Role of Immune cells in Thrombi of Acute Stroke Patients: A Novel Approach Through Spatial Transcriptomics

Ok, Taedong

Department of Medicine

Graduate School

Yonsei University

Deciphering the Role of Immune cells in Thrombi of Acute Stroke Patients: A Novel Approach Through Spatial Transcriptomics

Advisor Lee, Kyung-Yul

A Dissertation Submitted
to the Department of Medicine
and the Committee on Graduate School
of Yonsei University in Partial Fulfillment of the
Requirements for the Degree of
Doctor of Philosophy in Medical Science

Ok, Taedong

June 2025

Deciphering the Role of Immune cells in Thrombi of Acute Stroke Patients: A Novel Approach Through Spatial Transcriptomics

This Certifies that the Dissertation of Ok, Taedong is Approved

`

Committee Chair	**Fang, Sungsoon**
Committee Member	**Lee, Kyung-Yul**
Committee Member	**Jung, Yo Han**
Committee Member	**Han, Sang Won**
Committee Member	**Bhin, Jinhyuk**

Department of Medicine
Graduate School
Yonsei University
June 2025

ACKNOWLEDGEMENTS

I would like to express my deepest gratitude to my thesis supervisor, Professor Kyung-Yul Lee, for his continuous guidance and encouragement throughout this research. I am also sincerely grateful to the esteemed members of my thesis committee, Professor Sungsoon Fang (Chair), Professor Yo Han Jung, Professor Sang Won Han, and Professor Jinhyuk Bhin, for their invaluable insights and constructive feedback.

Additionally, I would like to acknowledge Sugyeong Jo for her significant contributions to this research. Lastly, I extend my heartfelt appreciation to my colleagues, friends, and family, whose support and encouragement have been instrumental in the completion of this dissertation.

TABLE OF CONTENTS

LIST OF FIGURES

LIST OF TABLES

ABSTRACT

Deciphering the Role of Immune cells in Thrombi of Acute Stroke Patients: A Novel Approach Through Spatial Transcriptomics

Cardioembolic (CE) and large artery atherosclerosis (LAA) strokes are major causes of acute ischemic stroke (AIS), with a high recurrence risk. Studies on thrombus composition in AIS subtypes have yielded conflicting results, underscoring the need for further investigation. Immune cells such as neutrophils and macrophages promote thrombosis in cardiovascular diseases, but their role in thrombosis across AIS subtypes remains unclear. Here, we employed spatial transcriptomics to investigate the molecular characteristics of immune cells within thrombi from AIS patients with LAA and CE. Molecular profiling revealed distinct immune activities despite no significant differences in immune cell presence by immunostaining. LAA thrombi exhibited a profibrotic profile with $CD163^{+}$ macrophages and upregulated TGF-β signaling. CE thrombi showed increased neutrophil activation and NET formation, with elevated CXCR4 expression. These findings suggest that targeting differential immune cell activation could provide etiology-specific therapeutic strategies to reduce recurrence and improve outcomes.

Key words : Spatial transcriptomics, ischemic stroke, etiology, thrombi, clots, thrombectomy

1. INTRODUCTION

Stroke ranks as one of the leading causes of mortality globally, with ischemic strokes comprising the majority of all new cases and resulting in approximately 63.48 million disability-adjusted life years and 3.29 million deaths annually.[1] Etiological diagnosis of acute ischemic stroke (AIS) subtypes, primarily using the TOAST (Trial of Org 10172 in Acute Stroke Treatment) classification, is crucial for developing effective strategies to prevent recurrence.[2] Anticoagulation therapy is typically prescribed for patients with cardioembolic (CE) strokes, based on the traditional understanding that this is primarily due to the formation of fibrin-rich clots in a hypercoagulable state as outlined by Virchow's triad.[3] Conversely, antiplatelet agents are favored for patients with large artery atherosclerosis (LAA) strokes, where thrombus formation involves platelet aggregation triggered by ruptured atherosclerotic plaques.[4]

In the last decade, endovascular thrombectomy (EVT) in patients with large vessel occlusion strokes has not only significantly improved clinical outcomes but also facilitated the histological, biochemical, and structural analysis of retrieved clots.[5-9] These analyses have shown that the composition of the thrombus, which includes red blood cells (RBCs), white blood cells (WBCs), fibrin, and platelets, is closely linked with AIS etiology, EVT recanalization rates, stroke severity, and functional outcomes.[10,11] Thrombi with higher RBC content are generally more deformable and porous, enabling easier device engagement and better penetration of tissue plasminogen activator (tPA), while clots rich in fibrin and platelets tend to be denser, more rigid, and less responsive to reperfusion therapies. Emerging evidence also suggests that neutrophil extracellular traps (NETs) contribute to thrombus stability and resistance to both enzymatic degradation and mechanical retrieval by forming compact, lytic-resistant structures. These compositional and structural differences have been variably linked to stroke subtypes, with fibrin- and platelet-dominant clots more frequently observed in CE strokes and RBC-rich clots in LAA strokes. However, literature remains inconsistent, with some studies reporting conflicting associations between thrombus composition and etiology.[12] As these molecular pathways are influenced by the mechanisms involved in clot formation, these inconsistencies emphasize the need to explore the pathways linked to specific cell types within thrombi.

Immunothrombosis links inflammation and the coagulation cascade, forming intravascular clots as a defense against infection or injury. However, aberrant activation in cardiovascular diseases like myocardial infarction and stroke leads to thrombotic disorders.[13] Platelets are key drivers of

immunothrombosis, contributing to thrombosis and activating innate immune cells such as neutrophils and monocytes. At sites of vascular injury, platelets adhere to the extracellular matrix and release agonists like ADP and thromboxane A_2, further releasing chemokines such as CXCL4 and CCL5, which recruit neutrophils.[14] Platelet-neutrophil interactions, via P-selectin and HMGB1, promote the formation of NETs, which serve as scaffolds for thrombus formation and are abundant in AIS thrombi.[15,16] NETs induce thrombin generation by activating coagulation factor XII. Monocytes also interact with platelets through PSGL-1 and Mac-1, forming aggregates that promote the release of pro-inflammatory cytokines like IL-1β and IL-6, further driving NET formation.[17,18] Despite the significant role of innate immune cells in thrombosis, research on thrombi in AIS has primarily focused on thrombus composition, limited by the difficulty in obtaining sufficient nucleated cells for analysis.[19,20] The low cellular yield and technical challenges in isolating cells from thrombi with high stiffness have made it hard to perform in-depth molecular studies. Bulk RNA sequencing, which is alternatively used, lacks the spatial resolution necessary to capture the cellular heterogeneity within thrombi, as it averages gene expression across entire samples. However, recent advancements in spatial transcriptomics technologies, such as GeoMx Digital Spatial Profiling (DSP), allow for cell-specific transcriptomic profiling. GeoMx preserves spatial context and targets specific cell populations within tissue sections using antibodies, enabling precise molecular analysis.

In this study, 42 ischemic stroke patients were enrolled, and retrieved thrombi were used to investigate distinct characteristics and the presence of innate immune cells. GeoMx DSP was employed to explore how immune cells contribute to thrombosis across different AIS etiologies. By analyzing different molecular signatures of immune cells between CE and LAA subtypes, we aim to provide insights into the immune mechanisms underlying thrombus formation in AIS.

2. MATERIALS AND METHODS

2.1. Ethics, Patient Recruitment and Sample Collection

This study was approved by the National Health Insurance Service (NHIS) Ilsan Hospital Institutional Review Board (IRB-2022-09-025). All procedures were conducted following the authorized protocol, and written consent was received from all participants.

We included patients who underwent EVT from December 2022 through July 2024 at NHIS

Ilsan Hospital, from whom sufficient size of thrombi for analysis were successfully retrieved. The retrieved thrombi were immersed in 4% paraformaldehyde for fixation immediately after EVT and stored until use.

2.2. Clinical Parameters, Stroke Etiology, and Sample Selection

Patients underwent regular assessments involving brain magnetic resonance imaging, and either magnetic resonance angiography or computed tomography angiography, heart examinations (such as echocardiography, 24-hour wearable EKG, and cardiac computed tomography), along with routine blood analyses. We collected clinical parameters including demographics (age and sex), underlying vascular risk factors (hypertension, diabetes mellitus, dyslipidemia, and smoking history), prior history of stroke, prior history of cardiac disease (coronary artery disease, atrial fibrillation, and heart failure) and stroke severity as per the National Institutes of Health Stroke Scale (NIHSS). Stroke etiology was classified based on Trial of Org 10172 in Acute Stroke Treatment (TOAST) classification. Eight specimens were selected for spatial transcriptomics analysis: four with LAA etiology and four with CE etiology. The initial selection was based on TOAST classification, followed by the identification of thrombus from patients that most accurately represented each etiology, informed by imaging and clinical data. This was done by an interventional neurologist (T.O.).

2.3. Histological, Immunohistochemistry and Immunofluorescence Staining

For histological analysis, retrieved thrombi were fixed in 4% paraformaldehyde, embedded in paraffin, and sectioned at 4 μM. The slides were stained with hematoxylin and eosin (H&E) and Masson's Trichrome. H&E staining was performed using Harris hematoxylin solution (merck HX29014375) and eosin Y (Sigma-Aldrich, E4382). Masson's Trichrome staining was performed using a Trichrome Stain Kit (Sigma-Aldrich, HT15).

For immunohistochemistry analysis, immunohistochemical staining was performed using formalin-fixed, paraffin-embedded (FFPE) thrombi. The 4 μM thick sections were deparaffinized in xylene and rehydrated through an ethanol gradient. Following deparaffination, antigen retrieval was facilitated by heating for 20 minutes with FLEX Target Retrieval Solution except for anti-CD42b

and anti-fibrinogen. The slides were then incubated for 10 minutes with a 3% hydrogen peroxide solution to inhibit endogenous peroxidase, followed by 2 washes with Tris-buffered saline. The slides were incubated with primary antibodies at room temperature for 1 hour and washed three times, followed by secondary antibody incubation at room temperature for 20 minutes with EnVision anti-mouse (Dako, K4001;) or EnVision anti-rabbit (Dako, K4003). The detection was performed with 3-3' diaminobenzidine (DAB) hydrochloride (DAKO, K3468) for 5 minutes. Counterstaining with hematoxylin for 10 min and mounting followed. Images were acquired with an automated slide scanner (Zeiss, Axioscan 7).

Deparaffinized sections from thrombi were heated at 95℃ in a FLEX Target Retrieval Solution (Dako, K8005) for 20 min. After antigen retrieval, 3% H_2O_2 solution was used for blocking endogenous peroxidase activity. The sections were incubated for 1 h at room temperature with primary antibodies: mouse anti-human ELA2 (Novus, MAB9167AF594, RRID: AB_3148269) and rabbit anti-human CXCR4 (Abcam, ab181020, RRID: AB_2910168). After washing, sections were incubated for 30 min at room temperature with secondary antibodies: donkey anti-rabbit AF488 (Invitrogen, A-21206, AB_2535792). Stained sections were mounted with Vectashield antifade mounting with DAPI (Vector Laboratories, H-1200, RRID: AB_2336790). Images were acquired with a laser scanning confocal microscope (Zeiss, LSM780).

Image analysis was performed using QuPath and ImageJ software by researchers who were blinded to the clinical information of the patients. The percentage of each thrombus component was quantified by measuring DAB-positive areas over total areas. The DAB images were acquired using a color deconvolution plugin and the positive area was calculated by an adjusted threshold according to the staining intensity of the respective antibody. The percentage of fibrosis was quantified from Masson's Trichrome stained images by measuring the blue-stained area over the total area.

2.4. Spatial Transcriptomics Analysis

The spatial transcriptomic profiles of acute ischemic thrombi were analyzed using GeoMx Digital Spatial Profiler (DSP). The 4 μM FFPE tissue sections were prepared and hybridized with the Human Whole Transcriptome Atlas (WTA) probes. The tissue slides were stained with fluorescent-labeled antibodies targeting an immune cell marker (CD45), macrophage markers (CD68, CD163), and neutrophil markers (ELA2, MPO), followed by Syto13 or Syto83 DNA nucleic acid staining. Details of the antibodies are provided in the Major Resources Table in the Supplemental Materials.

After staining, the slides were scanned using the GeoMx DSP instrument and regions of interest (ROIs) were selected based on immunofluorescence signals. Oligonucleotides from selected ROIs were released by ultraviolet light, then indexed using Illumina adapters. Libraries were sequenced at 100 bp paired-end on Illumina NovaSeq6000.

Each ROI's data was normalized by Q3 value and log-transformed normalized counts were used for the analyses. Differentially expressed genes (DEGs) between CE subtype and LAA subtype were identified with the following parameters: Benjamini–Hochberg adjusted P-value < 0.05 and fold change 1.5. Gene set enrichment analysis (GSEA) was performed using the GSEA software (version 4.2.3, Broad Institute). Hallmark and reactome gene sets were obtained from the molecular signatures database MSigDB (version 2024.1.Hs).[21,22] The gene set permutation number was set to 1000 for all analyses. Normalized enrichment score (NES) ≥ 1, nominal P-value <0.05 were considered as significant enrichment. NET score was calculated by the gene set variation analysis (GSVA) R package (version 1.52.3).[23] Previously identified neutrophils and NETosis-related gene sets were used to assess an enrichment score.[24,25]

2.5. Statistical Analysis

Statistical analysis was performed using R statistical software (version 4.4.1, R Core Team 2024) or with SPSS (version 30.0, IBM). The unpaired t-test was used to compare means between groups. For data not fitting a normal distribution or two independent groups, the Wilcoxon rank sum test was utilized. Ratios were compared using Pearson's chi-square test. P-value < 0.05 was considered statistically significant.

3. RESULTS

3.1. Baseline Characteristics of AIS patients

From December 15, 2022, to July 31, 2024, a total 42 AIS patients who underwent mechanical thrombectomy were recruited, and their thrombi were collected for this study. The clinical characteristics of patients (median age, 73.1±12.6 years; men, 54.8%) are presented in Table 1. Hypertension was the most prevalent vascular risk factor, affecting 25 patients (60%), followed by dyslipidemia (48%) and a history of smoking (36%), while diabetes mellitus was observed in 10 patients (24%). Among cardiac comorbidities, atrial fibrillation was the most common, present in

26 patients (62%), followed by coronary artery disease, heart failure, and valvular heart disease. At admission, 14 patients (33%) were on antiplatelet therapy, 5 (12%) were on anticoagulants, and 17 (41%) were on statin. Lipid profile analysis showed mean levels of total cholesterol (155.1 ± 43.7 mg/dL), triglycerides (133.8 ± 154.1 mg/dL), HDL-cholesterol (45.8 ± 13.9 mg/dL), and LDL-cholesterol (88 ± 35.2 mg/dL). The mean HbA1c was 5.9 ± 0.8%, with apolipoprotein A1 and B levels at 121.2 ± 27.5 mg/dL and 77.5 ± 26.4 mg/dL, respectively. Stroke characteristics revealed a median NIHSS score on admission of 15 (IQR 8.25–19). Most patients had occlusions in the ICA or MCA (45% each). The AIS etiologies were classified as 27 patients (64%) with CE stroke, 8 patients (19%) with LAA stroke, and 7 patients (17%) with cryptogenic stroke. Representative imaging findings of CE and LAA stroke are shown in Figure 1.

Table 1. Clinical Characteristics of Enrolled Patients

Parameter	Value
Demographics	
Age (years, mean ± SD)	73.1 ± 12.6
Sex, male	23 (54.8%)
Vascular Risk Factors	
Hypertension (HTN)	25 (60%)
Diabetes Mellitus (DM)	10 (24%)
Dyslipidemia	20 (48%)
Smoking	15 (36%)
Cardiac Diseases	
Coronary Artery Disease	12 (29%)
Valvular Heart Disease	7 (17%)
Atrial Fibrillation	26 (62%)
Heart Failure	8 (19%)
Medication at Admission	
Antiplatelet	14 (33%)
Anticoagulant	5 (12%)

Parameter	Value
Statin	17 (41%)
Lipid Profiles (mg/dL, mean ± SD)	
Total Cholesterol	155.1 ± 43.7
Triglyceride	133.8 ± 154.1
HDL-Cholesterol	45.8 ± 13.9
LDL-Cholesterol	88 ± 35.2
HbA1c (%)	5.9 ± 0.8
Apolipoprotein A1	121.2 ± 27.5
Apolipoprotein B	77.5 ± 26.4
Stroke Characteristics	
Initial NIHSS Score (median, IQR)	15 (8.25–19)
IV tPA	14 (33%)
Site of Occlusion	
Internal Carotid Artery (ICA)	19 (45%)
Middle Cerebral Artery (MCA)	19 (45%)
Basilar Artery (BA)	3 (7%)
Posterior Cerebral Artery (PCA)	1 (2%)
Etiology	
Cardioembolic (CE)	27 (64%)
Large Artery Atherosclerosis (LAA)	8 (19%)
Cryptogenic	7 (17%)

HTN: hypertension; DM: diabetes mellitus; HbA1c: glycated hemoglobin; NIHSS: National Institutes of Health Stroke Scale; IQR: interquartile range; IV: intravenous; tPA: tissue plasminogen activator; ICA: internal carotid artery; MCA: middle cerebral artery; BA: basilar artery; PCA: posterior cerebral artery.

Cardioembolic stroke

(A) Pre-thrombectomy (B) Post-thrombectomy

Large artery atherosclerosis stroke

(C) Pre-thrombectomy (D) Post-thrombectomy

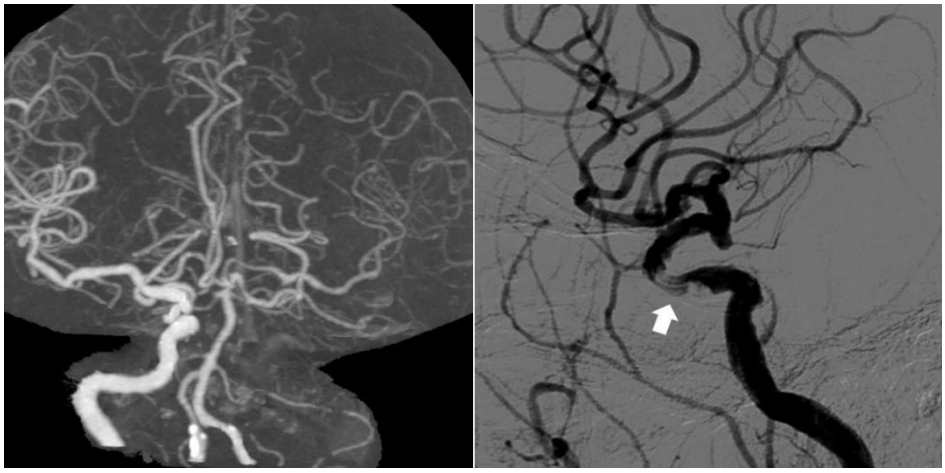

Figure 1. Representative imaging findings of cardioembolic and large artery atherosclerosis stroke. (A and B) Representative imaging findings of a cardioembolic stroke. (A) Brain computed tomography angiography showing occlusion of the right middle cerebral artery before mechanical thrombectomy. (B) Angiogram demonstrating successful recanalization of the right middle cerebral artery without residual stenosis. The cut-off sign at the right middle cerebral artery (white circle) is indicative of cardioembolism.
(C and D) Representative imaging findings of a stroke due to large artery atherosclerosis. (C) Brain

computed tomography angiography showing left internal carotid artery occlusion before mechanical thrombectomy. (D) Angiogram illustrating recanalization of the left internal carotid artery with a residual stenotic lesion (white arrow), suggestive of intra-arterial thrombosis secondary to atherosclerosis.

3.2. Immune Cell Profiling in Thrombi

To investigate the thrombus components of the two main AIS subtypes, CE and LAA, immunohistochemical (IHC) staining was conducted. Quantification of the primary components, including platelets, fibrin, and RBCs, showed that fibrin and RBCs constituted a larger proportion of thrombus composition in both subtypes compared to other components (Figure 2A and 2B); however, there were no significant differences in the proportions of these components between the CE and LAA subtypes (Figure 2C). The median percentage of fibrin was 63.43% (IQR 48.81–72.34%) in CE and 54.48% (IQR 45.41–66.62%) in LAA. For platelets, the median percentage was 39.88% (IQR 22.74–58.58%) in CE and 41.18% (IQR 29.96–62.52%) in LAA, with no significant differences found between the two subtypes. To confirm the presence of innate immune cells within thrombi, markers such as CD45, neutrophil elastase (NE) and citrullinated histone 3 (cit-H3), CD68 and CD163 were also assessed through IHC staining. For neutrophil and NET analysis, NE and cit-H3 were used. The median percentage of NE was 20.83% (IQR 14.20–38.88%) in CE and 22.27% (IQR 11.42–48.51%) in LAA, showing no significant difference between the two subtypes. Similarly, the median percentage of cit-H3 was 29.89% (IQR 14.40–89.45%) in CE and 12.97% (IQR 6.84–80.15%) in LAA, with no significant differences observed. For macrophages, CD68 and CD163 markers were used, with no significant differences in their content observed between the two etiologies. The median percentage of CD68 was 20.44% (IQR 7.26–37.20%) in CE and 14.32% (IQR 9.90–31.39%) in LAA, while CD163 was 10.33% (IQR 5.52–21.91%) in CE and 8.95% (IQR 4.20–36.28%) in LAA, respectively. These results suggest that differences in molecular characteristics, rather than immune cell composition, are more important between etiologies.

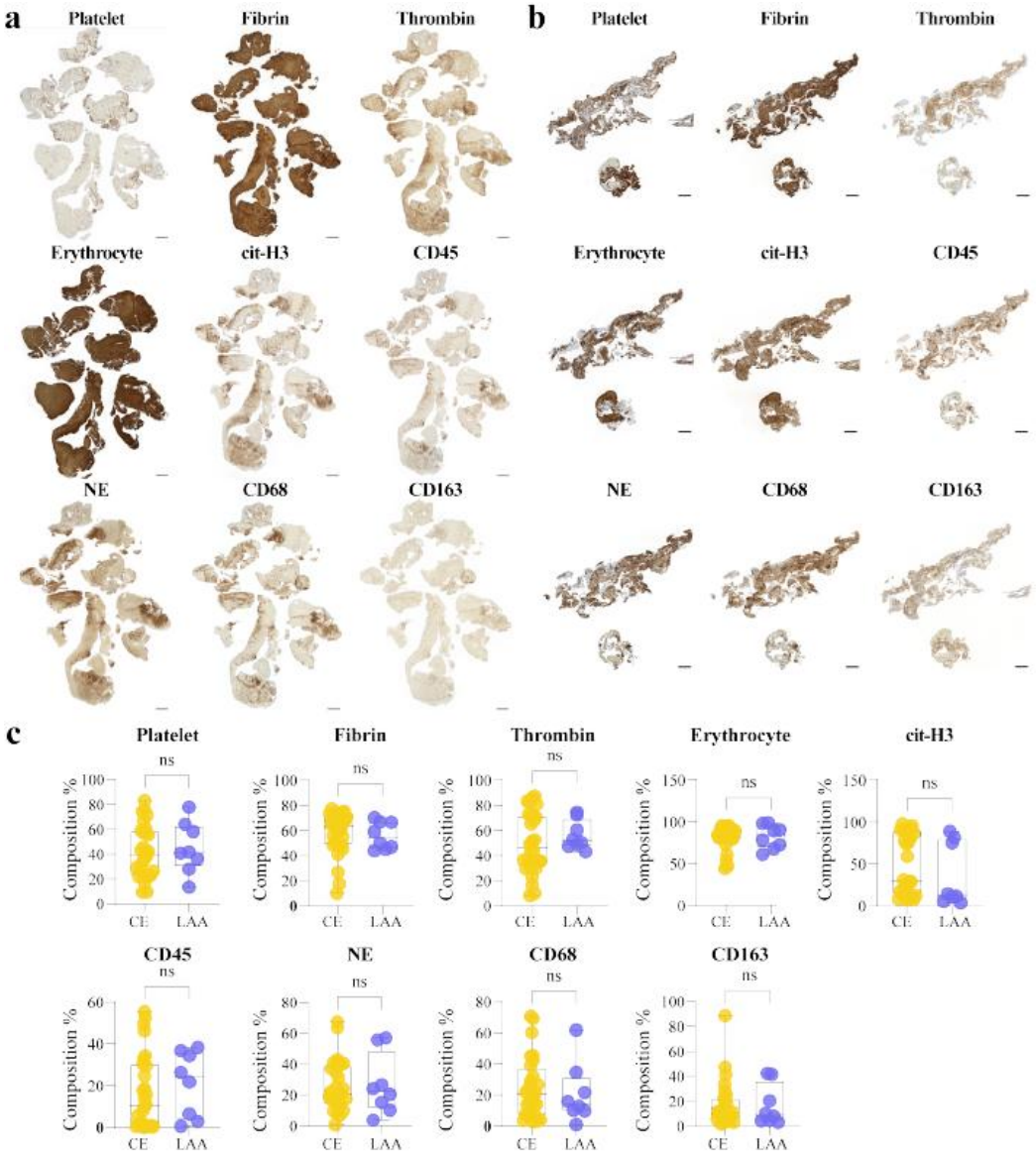

Figure 2. IHC analysis reveals no significant differences in the expression levels of thrombus components between CE and LAA subtypes. A and B, Representative images of IHC staining for platelet, fibrin, thrombin, erythrocyte, cit-H3, CD45, NE, CD68, and CD163 in CE thrombi (A) and LAA thrombi (B). Scale bars, 1 mm and 500 μm. C, Quantitative results of IHC staining for platelet, fibrin, thrombin, erythrocyte, cit-H3, CD45, NE, CD68, and CD163 in CE thrombi (n

= 27) and LAA thrombi (n = 8). Box-and-whisker plot shows the median, 25th and 75th percentiles, and whiskers show the minimum to maximum. Student's t test. ns, not significant.

3.3. Neutrophil Activation in CE Thrombi

To investigate the relationship between the immune cell expression profile in thrombi and AIS etiologies, GeoMx DSP was conducted using FFPE thrombi. (Figure 3A) Four thrombi from each CE and LAA subtype were retrieved for analysis. The samples were stained with innate immune cell markers and regions of interest (ROIs) containing more than 100 nuclei were selected to ensure high-quality transcriptome data. For specific analysis of activated neutrophils, samples were stained with NE and myeloperoxidase (MPO). A total of 24 ROIs in eight samples were selected. Segmentation was performed in these ROIs, focusing on NE+ MPO+ cells to target the activated neutrophil population. (Figure 3B) We then performed differential gene expression analysis of NE+ MPO+ segments to compare gene expression between the CE and LAA subtypes. There were 1,255 significant differentially expressed genes (DEGs) between CE and LAA. 1106 genes were significantly upregulated in CE samples. (Figure 3C)

Activated neutrophils release NETs, which contribute to thrombus formation by promoting coagulation and platelet activation.[26] To assess the difference in neutrophil activation between the two etiologies, we calculated the NET score using previously reported NET-related genes.[24,25] The neutrophil NET score was significantly higher in the CE subtype. (Figure 3D) Consistent with this result, we observed that G0S2, which is expressed in activated mature neutrophils, was most upregulated in the CE subtype. In addition, upregulation of genes involved in neutrophil chemotaxis (CXCR4, CXCL8, CXCL3) and neutrophil activation (NOX1, S100A12, TREM1) were identified in the CE subtype. In particular, CXCR4^hi neutrophils drive thrombosis in cardiovascular disease by promoting platelet production.[27] Immunofluorescence analysis confirmed CXCR4 overexpression in the CE subtype compared to LAA. (Figure 3E) Furthermore, gene set enrichment analysis (GSEA) of Reactome pathways revealed that platelet homeostasis and thrombin signaling through proteinase activated receptors (PARs) were enriched in the CE subtype. (Figure 3F) Overall, these results indicate that neutrophils are more activated in the CE subtype, leading to increased thrombus formation through enhanced NET release and platelet activation.

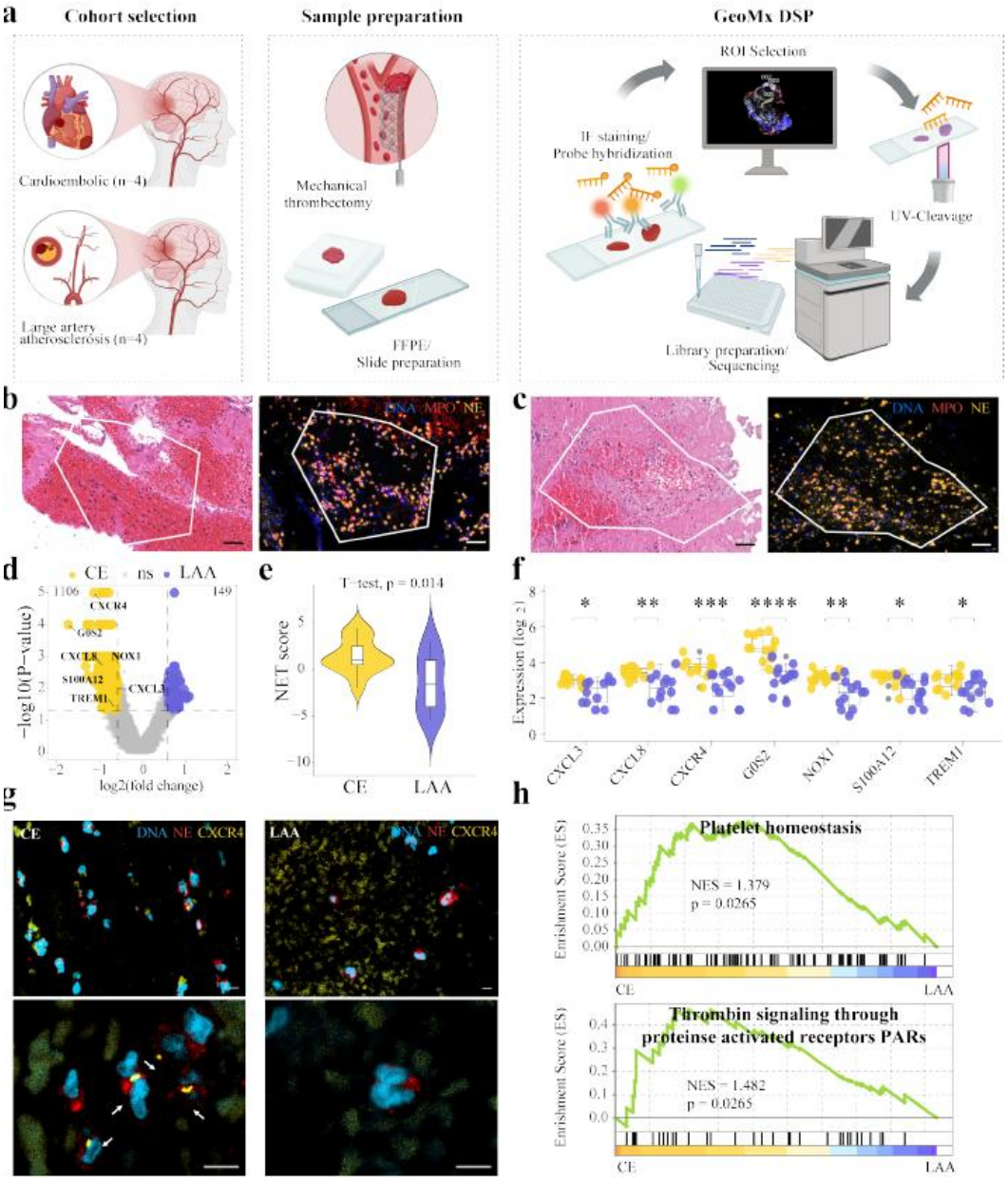

Figure 3. GeoMx spatial profiling reveals neutrophil activation and NET formation in CE thrombi. A, Schematic representation of the study workflow, including thrombus retrieval, section preparation, and GeoMx Digital Spatial Profiling (DSP). B, Representative images of the H&E-stained sections and corresponding immunofluorescence staining for DNA, NE, and MPO,

showing the ROIs for neutrophils in CE thrombi (left) and LAA thrombi (right). Scale bar, 50 μm. C, Volcano plot showing DEGs in NE+ MPO+ regions between CE thrombi and LAA thrombi ($p < 0.05$ and FC > 1.5). D, Violin plot of NET score on NE+ MPO+ regions. Student's t test (left). Box plots showing differential expressions of NET-related genes. Student's t test (right). E, Representative images of immunofluorescence staining for DAPI (blue), NE (red), and CXCR4 (yellow) in CE thrombi (left) and LAA thrombi (right). Scale bars, 5 μm. F, GSEA enrichment plots for "platelet homeostasis" and "thrombin signaling" gene sets enriched in NE+ MPO+ regions of CE thrombi. ∗$p < 0.05$; ∗∗$p < 0.01$; ∗∗∗$p < 0.001$; ∗∗∗∗$p < 0.0001$.

3.4. Profibrotic Characteristics in LAA Thrombi

To explore the distinct transcriptomic profiles of macrophages in thrombi from the CE and LAA subtypes, four samples from each subtype were stained with CD45, $CD68^+$, and $CD163^+$. A total of 28 ROIs were selected based on CD45 expression and further segmented into $CD68^+$ (CE, n = 7; LAA, n = 7) and $CD163^+$ (CE, n = 7; LAA, n = 7) groups. (Figure 4A and 4B) We then performed differential gene expression analysis by comparing $CD68^+$ macrophages between the CE and LAA subtypes and separately comparing $CD163^+$ macrophages between CE and LAA subtypes. (Figure 4C and 4D) A total of 958 significant DEGs ($p < 0.05$, FC > 1.5) were identified in $CD68^+$ macrophages, with 319 genes upregulated in the LAA subtype and 639 genes upregulated in the CE subtype. For $CD163^+$ macrophages, 1,298 significant DEGs were identified, with 629 genes upregulated in the LAA subtype and 669 genes in the CE subtype. For example, lipid droplet associated PLIN2 was significantly upregulated in $CD68^+$ macrophages of LAA subtypes, suggesting these macrophages are involved in differentiation into foam cells or exhibit enhanced lipid accumulation. (Figure 4E) In addition, TIMP, VCAN, and VIM were significantly upregulated in both $CD68^+$ and $CD163^+$ macrophages of the LAA subtype compared to the CE subtype, suggesting their involvement in the fibrosis-related processes within the LAA thrombi. (Figure 4E and 4F)

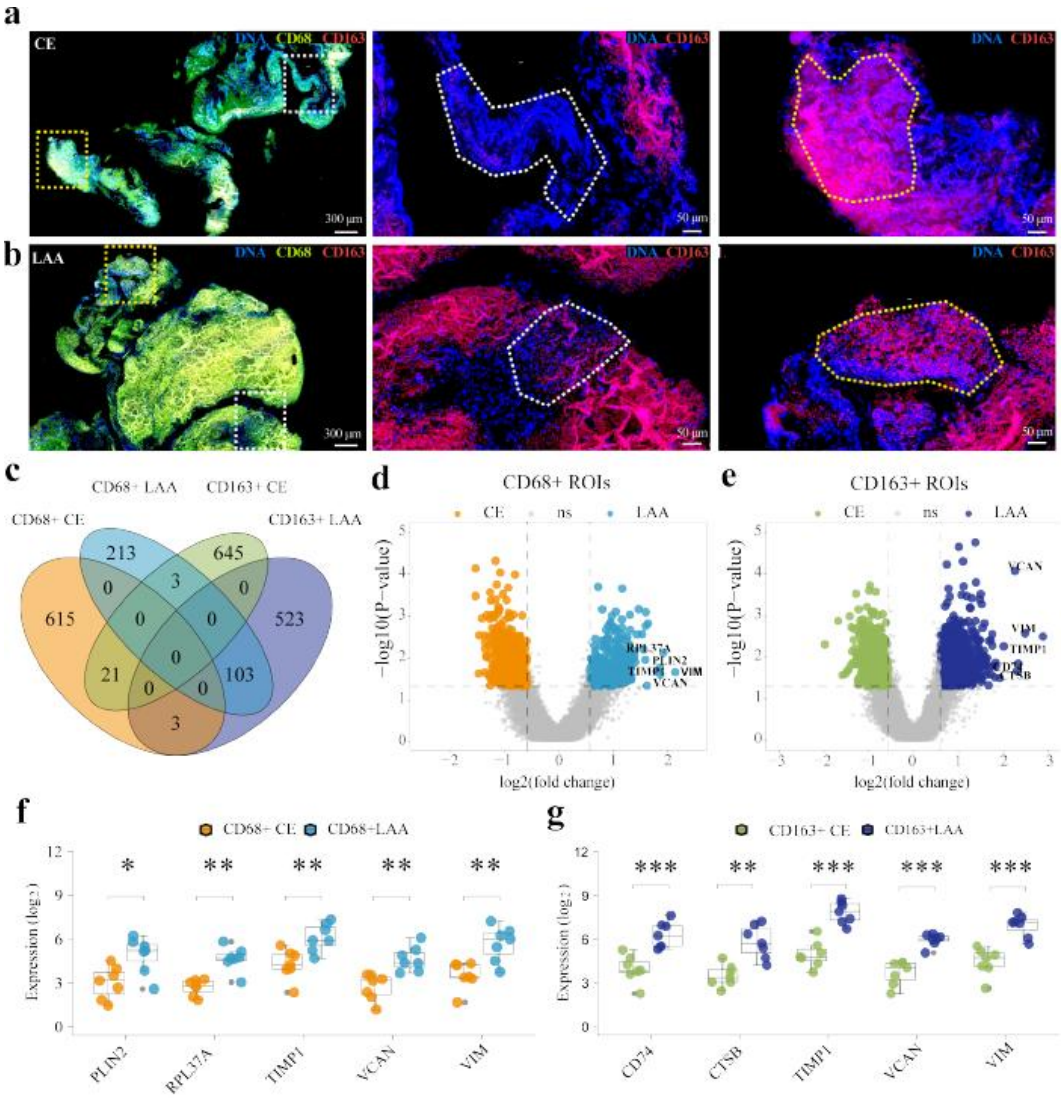

Figure 4. Spatial transcriptomic analysis reveals profibrotic characteristics of macrophages in LAA thrombi compared to CE thrombi. A and B, Representative images of immunofluorescence staining for DNA (blue), CD68 (green), and CD163 (red) in CE thrombus (A) and LAA thrombus (B). White dotted regions indicate areas of $CD68^+$ macrophages, and yellow dotted regions indicate areas of $CD163^+$ macrophages. Scale bars, 50 μm. C, Venn diagram showing the distribution of differentially expressed genes (DEGs) in $CD68^+$ and $CD163^+$ macrophages across CE and LAA thrombi ($p < 0.05$ and $FC > 1.5$). D, Volcano plots showing DEGs in $CD68^+$ (left) and $CD163^+$ (right)

macrophages between CE and LAA subtypes ($p < 0.05$ and FC > 1.5). E and F, Box plots of top-upregulated genes in $CD68^+$ (E) and $CD163^+$ (F) macrophages of LAA subtypes. Student's t test. $*p < 0.05$; $**p < 0.01$; $***p < 0.001$.

We performed GSEA analysis using the Hallmark Gene Sets to further explore functional differences of macrophages between the CE and LAA subtypes. (Figure 5A and 5B) Pathways including MYC_TARGETS_V1, TNFA_SIGNALING_VIA_NFKB, and PI3K_AKT_MTOR_SIGNALING were associated with both $CD68^+$ and $CD163^+$ macrophages of the LAA subtype. The INFLAMMATORY_RESPONSE pathway was among the top pathways in $CD68^+$ macrophages of the LAA subtype. In contrast, the INTERFERON_GAMMA_RESPONSE, OXIDATIVE_PHOSPHORYLATION, and TGF_BETA_SIGNALING pathways were specifically enriched in $CD163^+$ macrophages of the LAA subtype. GSEA analysis for Reactome pathways revealed that platelet activation, signaling and aggregation were enriched in both $CD68^+$ and $CD163^+$ macrophages of the LAA subtype, suggesting these macrophages promote thrombus formation in LAA by interacting with platelets. (Figure 5C)

The TGF-β signaling pathway is closely associated with fibrosis, promoting fibroblast activation and inducing endothelial to mesenchymal transition.[28] Notably, the TGF-β signaling pathway was identified as one of the pathways in $CD163^+$ macrophages of the LAA subtype. (Figure 5B) $CD163^+$ macrophages of the LAA subtype exhibited significantly higher expression of genes involved in the TGF-β signaling pathway (TGFB1, TGFBR2, TGFBI) compared to both $CD68^+$ macrophages from the CE and LAA subtypes and $CD163^+$ macrophages from the CE subtype. (Figure 5D and 5E) Additionally, we observed significantly elevated expression of FN1, a gene associated with profibrotic macrophages, in $CD163^+$ macrophages of the LAA subtype. Consistent with these results, Masson's trichrome staining demonstrated increased fibrosis in LAA thrombi compared to CE thrombi, suggesting a prominent role for $CD163^+$ macrophages in driving fibrosis within the LAA subtype. (Figure 3F)

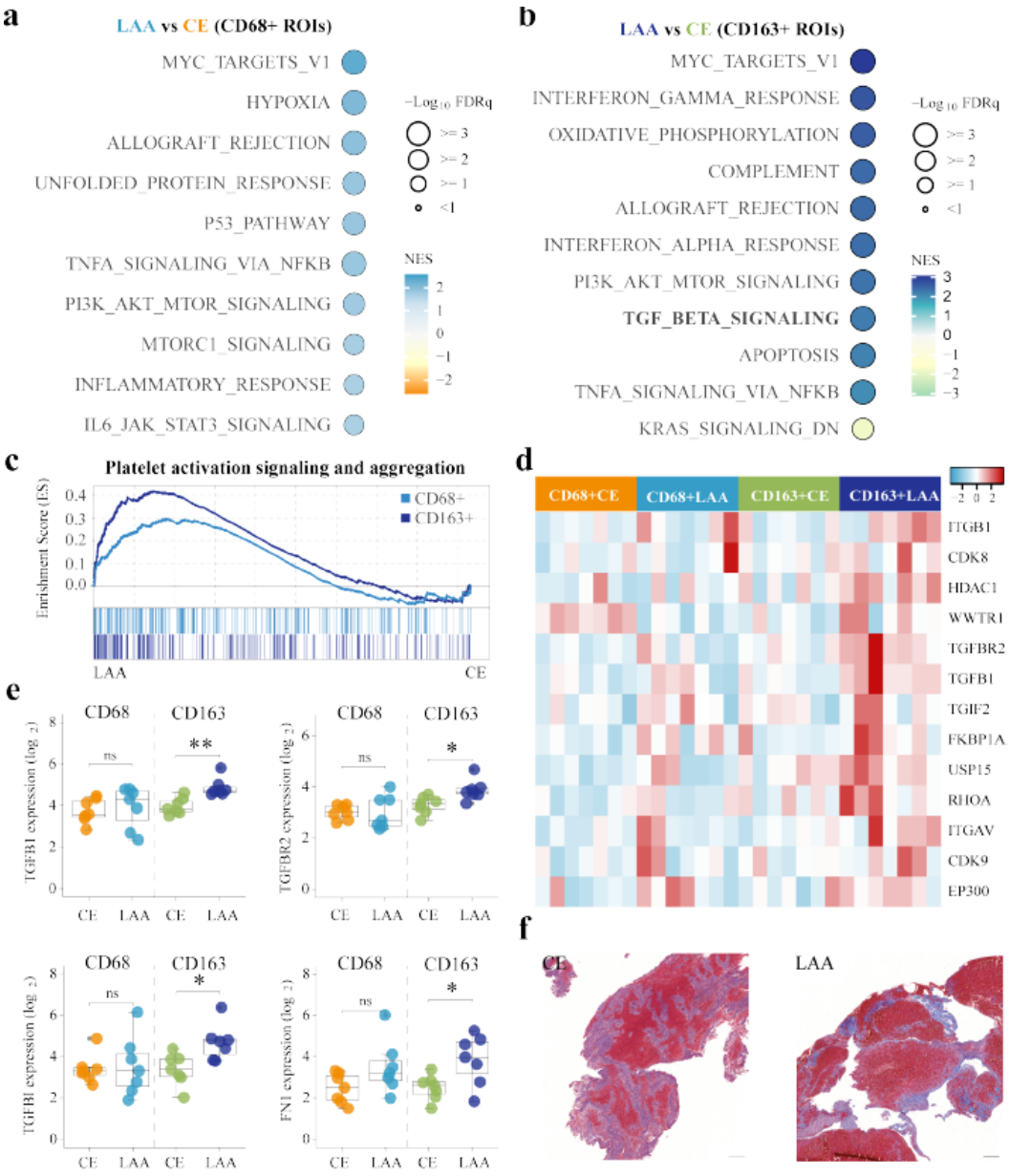

Figure 4. TGF-β signaling and profibrotic gene expression are enriched in CD163⁺ macrophages of LAA subtypes. A and B, Bubble plots of top up- and downregulated GSEA of hallmark pathways in CD68⁺ (A) and CD163⁺ (B) macrophages in LAA subtypes. C, GSEA enrichment plots of "platelet activation, signaling and aggregation" pathways in CD68⁺ and CD163⁺

macrophages, with higher enrichment observed in LAA thrombi. D, Heatmap of TGF-β signaling-related gene expression in $CD68^+$ and $CD163^+$ macrophages across CE and LAA subtypes. E, Box plots showing expression levels of TGF-β signaling-related genes in $CD68^+$ and $CD163^+$ macrophages across CE and LAA subtypes. Student's t test. F, Representative images of Masson's trichrome staining for fibrosis in CE and LAA thrombi. Scale bars, 200 μm. ns, not significant; $*p < 0.05$; $**p < 0.01$.

4. DISCUSSION

Antithrombotic agents have been prescribed based on AIS etiology, with anticoagulants often used for CE stroke and antiplatelet agents for non-CE stroke such as LAA stroke.[2,4] However, these strategies remain largely empirical, and the high recurrence rate of AIS is still challenging despite these interventions. Most previous studies on thrombosis mechanisms in AIS subtypes have focused on major component differences, such as fibrin, platelets, and RBCs. Due to the inherent characteristics of thrombi, these studies have been limited to IHC and bulk transcriptomic analyses, often yielding controversial results.[12,29-31] Recent advancements in spatial transcriptomics now enable more precise, cell-specific analyses of the molecular mechanisms involved in thrombosis. In this study, we analyzed thrombi from AIS patients who underwent mechanical thrombectomy to investigate molecular differences and underlying mechanisms between the two major etiologies, CE and LAA. In CE stroke, blood stasis, structural changes in the cardiac chamber, and abnormal changes in blood constituents initiate the coagulation cascade, leading to embolic thrombus formation, while in LAA stroke, inflammation destabilizes plaques, resulting in rupture and atherothrombosis.[3,32,33] We identified no significant differences in major thrombus components between the subtypes via IHC analysis of thrombi. Additionally, while innate immune cells involved in immunothrombosis were detected, their proportions did not differ notably. However, immune cell-specific activity analysis using GeoMx DSP revealed that CE thrombi are characterized by increased neutrophil activation and NET formation, whereas LAA thrombi exhibits a distinct macrophage-driven profibrotic profile.

A recent study by Walker, M. et al. demonstrated elevated neutrophil degranulation in CE thrombi using spatial transcriptomic profiling of $CD45^+$ leukocytes.[34] NETs are known to promote arterial thrombosis by providing scaffolds that trap platelets and RBCs. Studies on AIS have frequently

reported NET markers in blood and cerebral thrombi, suggesting DNase as a potential thrombolytic agent.[35-37] However, findings on NET content in AIS thrombi across different subtypes have been inconsistent. Genchi, A. et al. and Jabrah, D. et al. reported that CE thrombi contain higher NET levels compared to other AIS subtypes.[38] In contrast, our study found no significant differences in the expression levels of NETs or neutrophils between LAA and CE thrombi, as quantified by IHC analysis of cit-H3 and NE. This suggests a need to explore differences in neutrophil activation rather than simply expression levels. While most previous studies have focused on histological or bulk transcriptomic analysis of thrombi, a recent study by Walker et al. utilized spatial transcriptomics on $CD45^+$ leukocytes in CE thrombi, providing preliminary insights into cell-specific immune activation. Similarly, our analysis identified CE thrombi showing significant upregulation of neutrophil activation including NET formation via spatial transcriptomic profiling of NE^+MPO^+ neutrophils. We also observed increased expression of NET-related genes, such as G0S2, CXCL8, and CXCR4, in CE thrombi. CXCR4^hi neutrophils, commonly defined as “aged” neutrophils, are known to exhibit enhanced NET formation and increased aggregation with platelets.[39-41] Therefore, high CXCR4 expression in neutrophils underscores the importance of aged neutrophils in the pathogenesis of CE stroke. Collectively, our findings of subtype-specific elevation of CXCR4 highlight the role of neutrophils in promoting thrombus formation and maintaining stability in CE stroke.

In addition to neutrophils, monocytes/macrophages are also associated with arterial thrombosis. In atherosclerosis, macrophages contribute to plaque instability and thrombus formation by differentiating into foam cells and forming necrotic cores, which increase the risk of plaque rupture.[42] However, the specific role of macrophages in thrombus formation following plaque rupture remains largely unstudied due to limitations in analyzing rigid thrombi. Recently, Jabrah et al. reported similar levels of $CD68^+$ macrophage expression in thrombi from both CE and LAA subtypes.[43] Consistent with this finding, our immunostaining analysis showed no significant differences in the presence of $CD68^+$ and $CD163^+$ macrophages between CE and LAA thrombi. To further investigate the transcriptomic differences of macrophages across thrombus etiologies, we applied spatial transcriptomic profiling targeting $CD68^+$ and $CD163^+$ macrophages. According to their transcriptomic characterization, profibrotic markers were notably increased in both macrophages in LAA thrombi compared to CE thrombi, suggesting a unique role for profibrotic macrophages in the progression of thrombosis in this etiology.

Notably, we identified upregulation of the TGF-β signaling pathway in CD163$^+$ macrophages within LAA thrombi. TGF-β is a well-known profibrotic factor that drives tissue fibrosis and endothelial–mesenchymal transition, promoting atherosclerosis.[44] Furthermore, platelet–macrophage interactions enhance TGF-β signaling, contributing to a fibrotic environment.[45,46] In line with this, we observed enriched pathways for platelet activation, signaling, and aggregation in CD163$^+$ macrophages within LAA thrombi. These findings indicate that platelet interactions enhance TGF-β signaling in this macrophage subset. Recently, Mai H. et al. reported that inhibition of TGF-β1 significantly prolonged thrombosis time in a mouse model.[47] Therefore, the elevated TGF-β signaling observed in LAA thrombi suggests that CD163$^+$ macrophages drive fibrotic remodeling, enhancing thrombus stability in this etiology. Collectively, our findings suggest therapeutic potential of targeting TGF-β1 signaling to modulate profibrotic macrophage activity and reduce thrombus stability in LAA stroke.

Only approximately 15% of patients with AIS are eligible for intravenous thrombolysis, and among those, successful reperfusion is achieved in less than half.[48,49] While factors such as excessive thrombus burden and thrombus location are known contributors to reperfusion failure, resistance to thrombolytic agents due to intrinsic thrombus characteristics is increasingly recognized as a critical factor. In our study, although we did not observe significant differences in the gross composition of thrombi between CE and LAA subtypes, distinct immunological and molecular profiles were evident. Previous studies suggest that thrombi with high fibrin content, regardless of stroke etiology, exhibit greater resistance to thrombolysis. Building on this, our results raise the possibility that adjunctive therapies targeting immune-related thrombus stabilization pathways could enhance recanalization efficacy. In CE patients, co-administration of thrombolytics with neutrophil-targeted interventions such as DNase or CXCR4 antagonists (e.g., AMD3100) may improve thrombolytic responsiveness. In LAA patients, given the observed enrichment of platelet activation pathways in CD163$^+$ macrophages, co-administration of thrombolytics with TGF-β1 inhibitors may offer a promising approach to overcome thrombolytic resistance.

Similarly, EVT achieves successful reperfusion in approximately 70–80% of cases.[50] While anatomical barriers may contribute to EVT failure, intrinsic thrombus properties—such as rigidity, friction, and immune-mediated resistance—also play a significant role. Previous studies have shown that bridging therapy with tPA prior to EVT improves reperfusion rates.[51-53] However, the use of tPA is limited by a narrow therapeutic window (within 4.5 hours of symptom onset) and an increased

risk of hemorrhage. Our findings highlight the potential for targeted, immune-modulating therapies—such as DNase or CXCR4 antagonists in CE and TGF-β1 pathway inhibition in LAA—to enhance reperfusion success, while possibly minimizing the risk of additional bleeding. These insights offer clinically meaningful opportunities to refine acute stroke treatment strategies and personalize reperfusion therapy based on thrombus biology.

One major limitation is the absence of in vivo animal models to validate the transcriptomic profiling results. The existing thrombosis model, the ferric chloride ($FeCl_3$)-induced thrombosis model, is not physiologically relevant.[54] In this model, thrombosis rapidly progresses within seconds, limiting their utility for detailed mechanistic investigations. Additionally, there are no established animal models which accurately reflect the specific subtypes of stroke, such as CE and LAA. While atherosclerosis models, including LDL receptor-deficient (LDLr−/−) and apolipoprotein E-deficient (apoE−/−) mice, are commonly used, these models do not reliably progress to thrombus formation.[55] Addressing these limitations in future studies will be essential for advancing our understanding of AIS pathophysiology and therapeutic strategies.

5. CONCLUSION

Our study highlights distinct immune cell-specific mechanisms in AIS subtypes. LAA thrombi exhibited a macrophage-driven profibrotic profile with upregulated TGF-β signaling, contributing to thrombus stability. In contrast, CE thrombi showed increased neutrophil activation and NET formation, associated with elevated CXCR4 expression. These findings suggest that targeting TGF-β1 signaling may offer promising therapeutic strategies for LAA strokes, while CXCR4 inhibition could benefit CE strokes, providing etiology-specific approaches to improve AIS outcomes.

References

1. G. S. Collaborators, ″Global, regional, and national burden of stroke and its risk factors, 1990–2019: a systematic analysis for the Global Burden of Disease Study 2019,″ *The Lancet Neurol.*, vol. 20, p. 795, 2021.
2. D. O. Kleindorfer, A. Towfighi, S. Chaturvedi, K. M. Cockroft, J. Gutierrez, D. Lombardi-Hill, H. Kamel, W. N. Kernan, S. J. Kittner, and E. C. Leira, ″2021 guideline for the prevention of stroke in patients with stroke and transient ischemic attack: a guideline from the American Heart Association/American Stroke Association,″ *Stroke*, 2021.
3. T. Watson, E. Shantsila, and G. Y. Lip, ″Mechanisms of thrombogenesis in atrial fibrillation: Virchow's triad revisited,″ *The Lancet*, vol. 373, pp. 155–166, 2009.
4. N. Kapil, Y. H. Datta, N. Alakbarova, E. Bershad, M. Selim, D. S. Liebeskind, O. Bachour, G. H. Rao, and A. A. Divani, ″Antiplatelet and anticoagulant therapies for prevention of ischemic stroke,″ *Clin. Appl. Thromb. Hemost*., vol. 23, pp. 301–318, 2017.
5. O. A. Berkhemer et al., ″A randomized trial of intraarterial treatment for acute ischemic stroke,″ *N. Engl. J. Med*., vol. 372, pp. 11–20, 2015.
6. B. C. Campbell et al., ″Endovascular therapy for ischemic stroke with perfusion-imaging selection,″ *N. Engl. J. Med*., vol. 372, pp. 1009–1018, 2015.
7. M. Goyal et al., ″Randomized assessment of rapid endovascular treatment of ischemic stroke,″ *N. Engl. J. Med*., vol. 372, pp. 1019–1030, 2015.
8. T. G. Jovin et al., ″Thrombectomy within 8 hours after symptom onset in ischemic stroke,″ *N. Engl. J. Med*., vol. 372, pp. 2296–2306, 2015.
9. J. L. Saver et al., ″Stent-retriever thrombectomy after intravenous t-PA vs. t-PA alone in stroke,″ *N. Engl. J. Med*., vol. 372, pp. 2285–2295, 2015.
10. S. Staessens et al., ″Studying stroke thrombus composition after thrombectomy: what can we learn?,″ *Stroke*, vol. 52, pp. 3718–3727, 2021.

11. S. Patil et al., ″Characterising acute ischaemic stroke thrombi: insights from histology, imaging and emerging impedance-based technologies,″ Stroke Vasc. Neurol., vol. 7, 2022.

12. P. B. Sporns et al., ″Ischemic stroke: what does the histological composition tell us about the origin of the thrombus?,″ *Stroke*, vol. 48, pp. 2206–2210, 2017.

13. K. Stark and S. Massberg, ″Interplay between inflammation and thrombosis in cardiovascular pathology,″ *Nat. Rev. Cardiol*., vol. 18, pp. 666–682, 2021.

14. S. Offermanns, ″Activation of platelet function through G protein–coupled receptors,″ *Circ. Res.*, vol. 99, pp. 1293–1304, 2006.

15. N. Maugeri et al., ″Activated platelets present high mobility group box 1 to neutrophils, inducing autophagy and promoting the extrusion of neutrophil extracellular traps,″ *J. Thromb. Haemost*., vol. 12, pp. 2074–2088, 2014.

16. C. Schulz and S. Massberg, ″Demystifying the prothrombotic role of NETs,″ *Blood*, vol. 129, pp. 925–926, 2017.

17. A. Weyrich et al., ″Monocyte tethering by P-selectin regulates monocyte chemotactic protein-1 and tumor necrosis factor-alpha secretion. Signal integration and NF-kappa B translocation,″*J. Clin. Invest*., vol. 95, pp. 2297–2303, 1995.

18. A. K. Meher et al., ″Novel role of IL (Interleukin)-1β in neutrophil extracellular trap formation and abdominal aortic aneurysms,″ *Arterioscler. Thromb. Vasc. Biol*., vol. 38, pp. 843–853, 2018.

19. G. Costamagna et al., ″Advancing Stroke Research on Cerebral Thrombi with Omic Technologies,″ *Int. J. Mol. Sci*., vol. 24, p. 3419, 2023.

20. N. Boodt et al., ″Mechanical characterization of thrombi retrieved with endovascular thrombectomy in patients with acute ischemic stroke,″ *Stroke*, vol. 52, pp. 2510–2517, 2021.

21. A. Liberzon et al., ″The molecular signatures database hallmark gene set collection,″ *Cell*

Syst., vol. 1, pp. 417–425, 2015.

22. D. Croft et al., "Reactome: a database of reactions, pathways and biological processes," *Nucleic Acids Res*., vol. 39, pp. D691–D697, 2010.

23. S. Hänzelmann, R. Castelo, and J. Guinney, "GSVA: gene set variation analysis for microarray and RNA-seq data," *BMC Bioinformatics*, vol. 14, pp. 1–15, 2013.

24. Y. Zhang et al., "A signature for pan-cancer prognosis based on neutrophil extracellular traps," J. Immunother. *Cancer*, vol. 10, 2022.

25. J. Wang et al., "NET-related gene signature for predicting AML prognosis," *Sci. Rep*., vol. 14, p. 9115, 2024.

26. C. Thålin et al., "Neutrophil extracellular traps: villains and targets in arterial, venous, and cancer-associated thrombosis," *Arterioscler. Thromb. Vasc. Biol*., vol. 39, pp. 1724–1738, 2019.

27. T. Petzold et al., "Neutrophil 'plucking' on megakaryocytes drives platelet production and boosts cardiovascular disease," *Immunity*, vol. 55, pp. 2285–2299, e2287, 2022.

28. N. G. Frangogiannis, "Transforming growth factor–β in tissue fibrosis," *J. Exp. Med*., vol. 217, 2020.

29. S. H. Ahn et al., "Histologic features of acute thrombi retrieved from stroke patients during mechanical reperfusion therapy," *Int. J. Stroke*, vol. 11, pp. 1036–1044, 2016.

30. T. Boeckh-Behrens et al., "Thrombus histology suggests cardioembolic cause in cryptogenic stroke," *Stroke*, vol. 47, pp. 1864–1871, 2016.

31. K. Maekawa et al., "Erythrocyte-rich thrombus is associated with reduced number of maneuvers and procedure time in patients with acute ischemic stroke undergoing mechanical thrombectomy," *Cerebrovasc. Dis. Extra*, vol. 8, pp. 39–49, 2018.

32. D. Fatkin, R. P. Kelly, and M. P. Feneley, "Relations between left atrial appendage blood flow velocity, spontaneous echocardiographic contrast and thromboembolic risk in vivo,"

J. Am. Coll. Cardiol., vol. 23, pp. 961–969, 1994.

33. L. Badimon and G. Vilahur, "Thrombosis formation on atherosclerotic lesions and plaque rupture," *J. Intern. Med*., vol. 276, pp. 618–632, 2014.

34. M. Walker, E. Federico, J. L. Espinoza, and C. L. Dupont, "Unveiling molecular diversity in cerebral thrombi via spatial transcriptomics," *Stroke*, vol. 55, pp. e266–e268, 2024.

35. T. Baumann et al., "Assessment of associations between neutrophil extracellular trap biomarkers in blood and thrombi in acute ischemic stroke patients," *J. Thromb. Thrombolysis*, pp. 1–11, 2024.

36. E. Laridan et al., "Neutrophil extracellular traps in ischemic stroke thrombi," *Ann. Neurol*., vol. 82, pp. 223–232, 2017.

37. C. Ducroux et al., "Thrombus neutrophil extracellular traps content impair tPA-induced thrombolysis in acute ischemic stroke," *Stroke*, vol. 49, pp. 754–757, 2018.

38. A. Genchi et al., "Cerebral thrombi of cardioembolic etiology have an increased content of neutrophil extracellular traps," *J. Neurol. Sci*., vol. 423, p. 117355, 2021.

39. C. Martin et al., "Chemokines acting via CXCR2 and CXCR4 control the release of neutrophils from the bone marrow and their return following senescence," *Immunity*, vol. 19, pp. 583–593, 2003.

40. C. Yang et al., "Aged neutrophils form mitochondria-dependent vital NETs to promote breast cancer lung metastasis," *J. Immunother. Cancer*, vol. 9, 2021.

41. K.-C. Ngamsri et al., "CXCR4 and CXCR7 inhibition ameliorates the formation of platelet–neutrophil complexes and neutrophil extracellular traps through Adora2b signaling," *Int. J. Mol. Sci*., vol. 22, p. 13576, 2021.

42. K. J. Moore and I. Tabas, "Macrophages in the pathogenesis of atherosclerosis," *Cell,* vol. 145, pp. 341–355, 2011.

43. D. Jabrah et al., "White blood cell subtypes and neutrophil extracellular traps content as biomarkers for stroke etiology in acute ischemic stroke clots retrieved by mechanical thrombectomy," *Thromb. Res*., vol. 234, pp. 1–8, 2024.

44. J. Ma, G. Sanchez-Duffhues, M.-J. Goumans, and P. Ten Dijke, "TGF-β-induced endothelial to mesenchymal transition in disease and tissue engineering," *Front. Cell Dev. Biol*., vol. 8, p. 260, 2020.

45. N. Song, K. Pan, L. Chen, and K. Jin, "Platelet derived vesicles enhance the TGF-beta signaling pathway of M1 macrophage," *Front. Endocrinol*., vol. 13, p. 868893, 2022.

46. K. Hoeft et al., "Platelet-instructed SPP1^{+} macrophages drive myofibroblast activation in fibrosis in a CXCL4-dependent manner," *Cell Rep*., vol. 42, 2023.

47. H. Mai et al., "Spatial proteomics analysis of soft and stiff regions in human acute arterial thrombus," *Stroke*, vol. 54, pp. 1636–1644, 2023.

48. GBD 2019 Stroke Collaborators, "Global, regional, and national burden of stroke and its risk factors, 1990–2019: a systematic analysis for the Global Burden of Disease Study 2019," *Lancet Neurol*, vol. 20, pp. 795–820, 2021.

49. D. O. Kleindorfer, A. Towfighi, S. Chaturvedi, et al., "2021 guideline for the prevention of stroke in patients with stroke and transient ischemic attack: a guideline from the American Heart Association/American Stroke Association," *Stroke*, vol. 52, pp. e364–e467, 2021.

50. N. Kapil, Y. H. Datta, N. Alakbarova, et al., "Antiplatelet and anticoagulant therapies for prevention of ischemic stroke," *Clin Appl Thromb Hemost*, vol. 23, pp. 301–318, 2017.

51. L. Gong, X. Zheng, L. Feng, et al., "Bridging therapy versus direct mechanical thrombectomy in patients with acute ischemic stroke due to middle cerebral artery occlusion: a clinical-histological analysis of retrieved thrombi," *Cell Transplant*, vol. 28, pp. 684–690, 2019.

52. D. Krajíčková, A. Krajina, I. Šteiner, et al., "Fibrin clot architecture in acute ischemic stroke treated with mechanical thrombectomy with stent-retrievers: a cohort study," *Circ*

J, vol. 82, pp. 866–873, 2018.

53. J. P. Bembenek, M. Niewada, J. Siudut, et al., "Fibrin clot characteristics in acute ischaemic stroke patients treated with thrombolysis: the impact on clinical outcome," *Thromb Haemost*, vol. 117, pp. 1440–1447, 2017.

54. T. Bonnard and C. E. Hagemeyer, "Ferric chloride-induced thrombosis mouse model on carotid artery and mesentery vessel," *J. Vis. Exp*., 2015.

55. G. S. Getz and C. A. Reardon, "Do the Apoe−/− and Ldlr−/−mice yield the same insight on atherogenesis?," *Arterioscler. Thromb. Vasc. Biol*., vol. 36, pp. 1734–1741, 2016.

Abstract in Korean

급성 뇌경색 환자의 혈전에서 면역세포의 역할 규명
: 공간 전사체 분석을 통한 새로운 접근

서론

급성 허혈성 뇌졸중(AIS)은 전 세계적으로 높은 이환율과 사망률을 보이는 질환이며, 심장성 색전증(CE)과 대동맥경화증(LAA)이 주요 원인이다. 두 아형은 혈전의 기원과 성상이 다르며, 이에 따라 항응고제와 항혈소판제 등 치료 전략이 구분된다. 그러나 병인에 따른 치료에도 불구하고 AIS 의 재발률은 여전히 높으며, 이는 혈전 내 면역세포의 역할이 명확히 밝혀지지 않았기 때문일 수 있다.

중성구와 대식세포는 혈전 형성 및 안정성에 관여하는 주요 면역세포로, 특히 중성구가 생성하는 NETs 와 대식세포의 섬유화 반응은 혈전의 성질에 큰 영향을 미친다. 본 연구는 공간 전사체 분석(Spatial Transcriptomics)을 통해 CE 와 LAA 혈전 내 면역세포 활성과 분자적 특성의 차이를 규명하고자 하였다.

연구방법

2022년 12월부터 2024년 7월까지 국민건강보험 일산병원에서 기계적 혈전제거술을 받은 AIS 환자 중 CE 또는 LAA 로 진단된 42명의 혈전을 분석 대상으로 하였다. 수술 후 채취된 혈전은 고정 및 포매 후 면역조직화학 염색(IHC)과 GeoMx 디지털 공간 전사체 분석(DSP)을 시행하였다.

IHC 에서는 혈전 내 섬유소, 혈소판, 적혈구 및 면역세포($CD45^+$, $CD68^+$, NE^+, $Cit\text{-}H3^+$)의 분포를 비교하였고, DSP 분석에서는 NE^+MPO^+ 중성구와 $CD68^+CD163^+$ 대식세포를 중심으로 아형 간 유전자 발현 차이를 평가하였다. 통계 분석은 R 프로그램을 이용하여 수행하였다.

연구결과

면역조직화학 분석 결과, CE와 LAA 혈전의 주요 성분(섬유소, 혈소판, 적혈구)과 면역세포의 비율에는 유의한 차이가 없었다. 이는 AIS 혈전이 조직학적으로는 병인에 따른 명확한 차이를 보이지 않을 수도 있음을 시사한다. 그러나 공간 전사체 분석을 통해 면역세포의 분자적 특성이 CE와 LAA 혈전 간에 현저한 차이를 보이는 것으로 나타났다.

CE 혈전에서는 중성구 활성화와 NET 형성이 증가하였으며, CXCR4, CXCL8, CXCL3 등의 유전자가 유의하게 상향 조절되었다. 특히 CXCR4는 '노화된(aged) 중성구'의 마커로, 혈소판 생성 및 혈전 형성을 촉진하는 역할을 한다. 본 연구에서도 CE 혈전에서 CXCR4가 과발현됨을 확인하였으며, 이는 중성구의 과활성이 CE 혈전의 주요 기전일 가능성을 시사한다.

반면, LAA 혈전에서는 $CD163^+$ 대식세포의 발현이 증가하였으며, TGF-β 신호전달 관

련 유전자(TGFB1, TGFBR2, TGFBI)의 발현이 유의하게 증가하였다. Masson's trichrome 염색 결과에서도 LAA 혈전에서 섬유화 조직이 증가한 것으로 나타났으며, 이는 $CD163^+$ 대식세포가 LAA 혈전의 구조적 안정성을 강화하는 데 기여할 가능성을 시사한다.

논의

본 연구는 CE와 LAA 혈전 내 면역세포 활성 차이가 혈전의 병리학적 특성에 중요한 영향을 미친다는 점을 시사한다. CE 혈전에서는 중성구 활성화와 NET 형성이 주요 기전으로 작용하며, LAA 혈전에서는 대식세포의 섬유화 반응이 혈전의 안정성을 증가시키는 것으로 나타났다.

이러한 결과를 바탕으로 AIS 치료 전략에 대한 새로운 병인 특이적 접근이 가능할 것으로 보인다. CE 뇌졸중에서는 NET 형성 억제제(DNase, PAD4 억제제) 또는 CXCR4 길항제(AMD3100)를 활용하여 중성구의 활성을 조절하는 전략이 고려될 수 있으며, LAA 뇌졸중에서는 TGF-β 신호 차단제(TGF-β1 억제제) 또는 항섬유화 치료를 병용하여 혈전 안정성을 낮추는 전략이 적용될 수 있다.

향후 본 연구에서 도출된 면역세포 활성 기전을 표적으로 하는 임상 연구가 수행된다면, CE 및 LAA 뇌졸중의 재발률을 낮추고, 환자의 예후를 개선할 수 있는 정밀의학적 접근법이 개발될 가능성이 있다.

결론

본 연구는 급성 뇌경색 환자의 CE 및 LAA 혈전에서 면역세포의 특성을 공간 전사체 분석을 통해 규명하였으며, 중성구 활성화와 NET 형성이 CE 혈전의 주요 특징이고, 대식세포의 섬유화 반응이 LAA 혈전의 병리적 특징임을 확인하였다. 이러한 결과는 AIS 환자의 병인 특이적 치료 전략 개발에 중요한 기초자료가 될 것으로 기대되며, 면역세포 조절을 통한 새로운 치료법의 가능성을 제시한다.

핵심되는 말 : 공간 전사체 분석, 허혈성 뇌졸중, 병인, 혈전, 응고, 혈전제거술